

Tight Binding Study of the Role of Charge Ordering in Colossal Magnetoresistive Manganites

S PANDA^{1†}, J K KAR² and G C ROUT³

¹Trident Academy of Technology, Chandaka Industrial Estate, Patia - 751024, Bhubaneswar, India.

²College of Engineering Bhubaneswar, Patia - 751024, Bhubaneswar, Odisha, India.

³Condensed Matter Physics Group, Physics Enclave, Plot No.- 664/4825, Lane-4A, Shree Vihar, Patia, Bhubaneswar -751031, Odisha, India. Email: gcr@iopb.res.in. Mob: 09937981694.

[†]Corresponding Author, Email: saswatip7@gmail.com

Received: 11.6.2016 ; Revised : 13.7.2016 ; Accepted :31.7.2016

Abstract. Doped rare-earth manganese oxides exhibit a rich phase diagram with a strong interplay between lattice, charge, spin and orbital degrees of freedom. We report here a tight binding model Hamiltonian consisting of AFM spin fluctuations in core band, double exchange interactions among conduction and core band electron spins and charge density wave interaction in the conduction band as an extra mechanism. The model Hamiltonian is solved using Zubarev's Green's function technique. The effect of first and second nearest neighbour interactions on thermal properties of manganite systems is studied.

Keywords: CMR, Charge orderings, antiferromagnetics, entropy

PACS Nos: 75.47.Gk, 71.30. Et, 75.50.Ee, 65.40.gd

1. Introduction

The perovskite manganese oxides have a general composition of $R_{1-x} A_x MnO_3$, where R and A are trivalent rare-earth and divalent alkaline earth ions respectively. These materials have been actively investigated over the past decades because of the colossal magnetoresistive (CMR) property [1] and its potential applications in magnetic data storage devices, magnetic sensors and spintronic devices. The manganese oxide compounds exhibit a complex phase diagram having varieties of electronic, structural and magnetic phases with

respect to doping concentration and temperature. These phase changes occur due to strong interplay between the lattice, charge, spin and orbital degrees of freedom. In the hole doped rare-earth manganites a thousand fold change in resistivity is observed on application of external magnetic field at insulating paramagnetic (PM) to conducting ferromagnetic (FM) transition temperature. For each hole doping, an Mn^{3+} ion is substituted by an Mn^{4+} ion. The presence of this mixed valent states along with double exchange (DE) mechanism gives rise to all the CMR phenomena observed in manganites. The DE mechanism was first proposed by Zener [2] in 1951. He proposed that the σ bonding orbitals on high spin Mn^{3+} ions is transferred to the empty σ bonding orbitals on Mn^{4+} ions by displacing electrons from the intermediate O^{2-} ions in a double exchange process: Mn^{3+} to O^{2-} to Mn^{4+} . Hund's interatomic exchange field would favour displacement of electrons with spins that were parallel to those on acceptor Mn^{4+} ions. This DE mechanism accounts for ferromagnetism and metallicity of the perovskite $\text{La}_{1-x}\text{Sr}_x\text{MnO}_3$. The fully quantum mechanical approach of DE interaction was proposed by Kubo and Ohata [3]. Using the s-d model Hamiltonian, the resistance and magnetoresistance (MR) are studied within the DE model at low temperatures. These calculations yield a metallic state above and below the Curie temperature. The DE models successfully explained the observed CMR effect near Curie temperature T_c qualitatively. But very low MR and wrong T_c were observed in comparison to the experimental values. So Millis et. al. [4] have suggested that there must be some extra mechanisms. The possible extra mechanisms are electron-phonon interaction, polaron, Jahn-Teller distortion and charge ordering. Millis et al. [4] proposed a DE model including electron-phonon coupling due to dynamic JT distortion. This leads to delocalization of charges as small polarons above the Curie temperature. T_c of such models agree with experimental results. The effect of JT coupling in terms of polarons and bipolarons was studied by Alexandrov et. al. [5]. The interaction of polaronic carriers with localized spins gives rise to a novel ferromagnetic transition along with collapse of carrier density. A highly anisotropic resistivity and a first order CMR phenomenon with an MR of $\sim 10000\%$ are observed for a two orbital DE model along with JT distortion [6]. Rout and co-workers have studied temperature dependent resistivity and metal-insulator (MI) phase transition considering JT distortion as an extra mechanism in presence of hybridization interaction [7] and DE interaction [8] among e_g and t_{2g} spins. As Mn^{3+} and Mn^{4+} ions sit at definite sites of the lattice, it leads to a super structure known as charge ordering (CO). The charge density wave (CDW) produces a gap and hence promotes an insulating phase. The doped carriers are ordered below

the CO temperature (T_{CO}) which is usually associated with orbital ordering (OO) and antiferromagnetism (AFM). The CO as an extra mechanism was first studied by Rout et. al. [9-13] in DE model. They have considered interplay between FM and CDW to explain the observed M-I transition and CMR effect near T_c through the study of temperature dependent magnetization [9], magnetic susceptibility [10], Raman spectra [11] and velocity of sound [12]. In all these studies they have got promising results. Further in the above model, they have included JT distortion as the second extra mechanism and studied the interplay between lattice, spin and charge degrees of freedom [13]. The ground state of manganese oxide compounds is an antiferromagnetic insulator. On doping a phase transition occurs from AFM to FM/PM. The FM phase is associated with metallicity. Though there are several experimental evidences of AFM phase, but theoretical study is not done extensively [1].

In the present communication we attempt here to study theoretically the role of CDW interaction on the thermal properties of CMR manganites. We have considered here the nearest neighbour and next nearest neighbour spin-spin Heisenberg interactions in the core d- electron levels in presence of double exchange interaction employed by Kubo and Ohata [3]. The DE and Heisenberg spin interactions are considered within mean-field approximation and the total Hamiltonian is solved by Zubarev's Green's function technique. The tight binding model Hamiltonian with first and second nearest neighbour hopping along with the calculation of mean-field parameters are presented in section 2. The results and discussion are presented in section 3 and finally the conclusion is written in section 4.

2. The Model

The model Hamiltonian is written as

$$\begin{aligned}
 H = & \sum_{k,\sigma} (\epsilon_k - \mu - B\sigma) c_{k,\sigma}^+ c_{k,\sigma} + \Delta_c \sum_{k,\sigma} c_{k,\sigma}^+ c_{k+Q,\sigma} \\
 & - J \sum_i S_i^d \cdot s_i^c - J_H \sum_{i,j} S_i^d \cdot S_j^d + \sum_{k,\sigma} (\epsilon_d - B\sigma) d_{k,\sigma}^+ d_{k,\sigma}
 \end{aligned}
 \tag{1}$$

In the model Hamiltonian, we consider the kinetic energies of e_g and t_{2g} band electrons, which are represented in first and last terms in the above equation. Here the terms ϵ_k , μ , B , σ and ϵ_d represent the e_g band dispersion energy, chemical potential, external magnetic energy, electron spin and position of core level with respect to Fermi level respectively. The second term represents the CDW interaction with Δ_c as the CDW gap and Q as the nesting wave vector.

The third term represents the Kubo - Ohata [3] type DE interaction among the e_g and t_{2g} spins at same site with DE coupling strength (J). The Heisenberg type spin exchange interaction in the core band with Heisenberg coupling constant J_H is given in the fourth term. The spin interactions given in the third and fourth terms in the Hamiltonian are treated within mean-field approximation. We have considered both nearest neighbour (NN) and next nearest neighbour (NNN) interactions in the e_g electron hoppings and the core electron spin interactions. As a result, the e_g electron band dispersion (ε_k) and the effective Heisenberg coupling appear as

$$\begin{aligned}\varepsilon_k &= -2t_1(\cos k_x + \cos k_y) - 4t_2(\cos k_x \cos k_y) \\ J_H &= J_1(\cos k_x + \cos k_y) + 2J_2 \cos k_x \cos k_y\end{aligned}$$

Further, transverse spin fluctuation is considered in the Heisenberg interaction. The mean-field Hamiltonian is solved using the Zubarev's Green's function technique [14] and both core and conduction band electron Green's functions are calculated. From the electron correlation functions, the temperature dependent average transverse spin fluctuation in t_{2g} band ($\langle S^d(t) \rangle$), e_g band ($\langle s^c(t) \rangle$) and the CDW gap parameters ($\Delta_c(t)$) are calculated using the following definitions.

$$\begin{aligned}\langle S^d(t) \rangle &= \frac{1}{N} \sum_k \langle d_{k,\uparrow}^+ d_{k,\downarrow} \rangle \\ \langle s^c(t) \rangle &= \frac{1}{N} \sum_k \langle c_{k,\uparrow}^+ c_{k,\downarrow} \rangle \\ \langle \Delta_c(t) \rangle &= -\sum_{k,\sigma} V_0 \langle c_{k,\sigma}^+ c_{k+Q,\sigma} \rangle\end{aligned}\tag{2}$$

The detail calculation of Green's functions, quasi particle energies ($\omega_{1,4}$) and order parameters are discussed in detail in the reference [13]. The e_g electron free energy per particle is written as $F = -k_B T \sum_{i,\alpha} \sum_{k,\sigma} \ln[1 + \exp(\beta \omega_{\alpha,k}^i)]$, where $\omega_{\alpha,k}^i$

are the quasi particle energies [15]. The electron entropy (S), specific heat (C_v) and Linear specific heat coefficients are calculated from the free energy. The order parameters given in equation (2) are solved numerically and self - consistently. The results thus obtained are used to study the thermal properties. All the physical parameters are made dimensionless after scaling with respect to the NN hopping integral t_1 . The reduced parameters are : the CDW coupling $g = V_0 N(0) / t_1$, the DE coupling $g_1 = J / t_1$, the NN Heisenberg coupling in t_{2g} band

$g_{1n} = J_1 / t_1$, the NNN Heisenberg coupling in t_{2g} band $g_{2n} = J_2 / t_1$ and the reduced temperature $t = k_B T / t_1$.

3. Results and Discussion

In the present microscopic model study of the interplay of antiferromagnetism (AFM) and charge ordering (CO), the transverse spin fluctuation ($\langle S^d(t) \rangle$) in core band and charge density wave (CDW) gap parameter (z) are solved self-consistently and numerically. The interplay of spin and charge degrees of freedom are studied by varying the nearest neighbour (NN) and next nearest neighbour (NNN) Heisenberg couplings, CDW and DE couplings in the study of AFM and CDW order parameters and temperature dependent entropy. The results obtained are discussed.

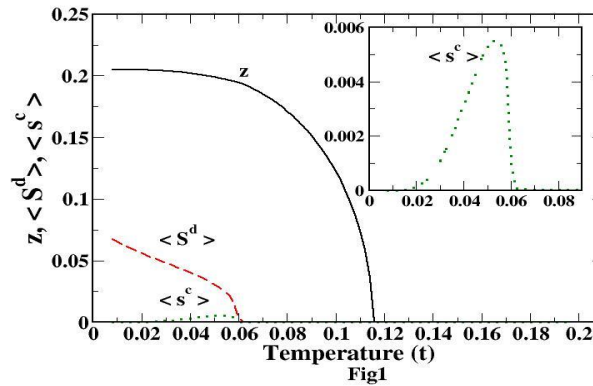


Fig.1. The temperature dependent self-consistency graphs of z , $\langle S^d \rangle$ and $\langle s^c \rangle$ for fixed values of $g = 1.08$, $g_1 = 2.5$, $g_{1n} = 6.72$, $g_{2n} = 0.25$, and $t_2 = 0.075$. Inset: the temperature dependent self-consistency graph of $\langle s^c \rangle$.

Figure1 shows the temperature dependent self-consistency graphs of average spin fluctuation in XY plane of core band ($\langle S^d(t) \rangle$), induced average transverse spin fluctuation in conduction band ($\langle s^c(t) \rangle$) and CDW gap (z) for a set of constant parameters $g = 1.08$, $g_1 = 2.5$, $g_{1n} = 6.72$, $g_{2n} = 0.25$ and $t_2 = 0.075$. The CDW gap parameter (z) shows a mean-field like behaviour with CDW transition temperature $t_{CDW} \approx 0.116$ ($T_{CDW} \approx 290K$). The AFM gap $\langle S^d(t) \rangle$ exhibits a first order phase transition with Neel temperature of $t_N = 0.06$ ($T_N \approx 150K$). A first order phase transition is observed in AFM spin fluctuation in XY plane in the experimental results for $Nd_{0.45} Sr_{0.55} MnO_3$ system [16] and model study of orbitally ordered manganites [17]. It is observed in several experiments that the charge ordering transition temperature $t_{CDW} < t_N$. The charge ordering transition

temperature and Neel temperature $T_{CDW} \approx 230$ K and $T_N \approx 152$ K for $La_{0.25}Ca_{0.75}MnO_3$ [18], $T_{CO} \approx 245$ K and $T_N \approx 175$ K for $Pr_{0.5}Ca_{0.5}MnO_3$ [19], $T_{CDW} \approx 235$ K and $T_N \approx 165$ k for $Pr_{0.63}Ca_{0.37}MnO_3$ [20] systems. The antiferromagnetism is induced in conduction band due to the presence of DE interaction between the core and conduction electron spins. The induced AFM spin fluctuation ($\langle s^c(t) \rangle$) has also the same Neel temperature as that of $\langle S^d(t) \rangle$. Below t_N , the $\langle s^c(t) \rangle$ increases and attains a maximum value at $t \approx 0.05$. On cooling down $\langle s^c(t) \rangle$ decreases rapidly and at very low temperatures, it is suppressed completely (see inset of figure 2(a)). This may be due to the presence of robust charge ordering at very low temperatures, as the charges get localized. Similar suppression in magnetization is observed for $Nd_{0.5}Sr_{0.5}MnO_3$ [21].

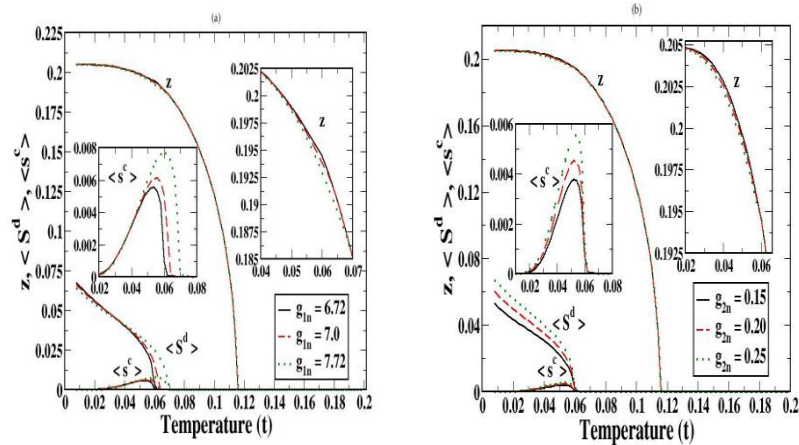


Fig.2(a). The temperature dependent self-consistency graphs of z , $\langle S^d \rangle$ and $\langle s^c \rangle$ for fixed values of $g = 1.08$, $g_1 = 2.5$, $g_{2n} = 0.25$, $t_2 = 0.075$ and for different values of $g_{1n} = 6.72, 7.0, 7.72$. Inset: the magnified temperature dependent self-consistency graph of $\langle s^c \rangle$ and z for different values of g_{1n} . **(b)** The temperature dependent self-consistency graphs of z , $\langle S^d \rangle$ for fixed values of $g = 1.08$, $g_1 = 2.5$, $g_{1n} = 6.72$, and $t_2 = 0.075$ and for different values of $g_{2n} = 0.15, 0.20, 0.25$. Inset: the temperature dependent self-consistency graph of $\langle s^c \rangle$ and z .

When the NN Heisenberg coupling strength, g_{1n} is increased from 6.72 to 7.72, the $\langle S^d(t) \rangle$ is enhanced near the Neel temperature and the Neel temperature is also enhanced (figure 2(a)). At lower temperatures, the $\langle S^d(t) \rangle$ decreases slightly with increase of g_{1n} . Crossing of the $\langle S^d(t) \rangle$ takes place at a temperature, $t \approx 0.035$, where $\langle s^c(t) \rangle$ is suppressed considerably. The $\langle s^c(t) \rangle$ does not show any variation with g_{1n} at low temperatures. However, the NN spin coupling g_{1n} substantially enhances the magnitude of the $\langle s^c(t) \rangle$ just near the magnetic transition temperature (t_N) where CMR effect in manganites is very

large. A small suppression in the CDW gap is observed in the temperature range where $\langle s^c(t) \rangle$ increases. Outside of which z remains unaffected. This indicates a strong interplay of charge and spin order parameters near the magnetic transition temperature. This may explain the observed CMR effect just below t_N . An interesting but different result is obtained by varying the NNN Heisenberg coupling g_{2n} (see figure 2(b)). With increase of g_{2n} from 0.15 to 0.25, the $\langle S^d(t) \rangle$ increases at lower temperatures. As one comes towards Neel temperature, this increase in $\langle S^d(t) \rangle$ becomes less and just below t_N , the $\langle S^d(t) \rangle$ remains constant (figure 2(b)) and the Neel temperature remains unaltered. As seen from temperature dependent $\langle s^c(t) \rangle$ curve, the $\langle s^c(t) \rangle$ also increases at lower temperatures, without any change near Neel temperature. As there is a strong competition between spin and charge orderings, the z decreases at lower temperatures. No change is observed in z with increase of g_{1n} above t_N , in the paramagnetic phase. It is seen that the NN Heisenberg coupling, g_{1n} is greater than the NNN Heisenberg coupling, g_{2n} . Though g_{2n} is small, its effect can not be ignored. Both NN and NNN Heisenberg couplings are important in stabilizing the magnetic order in manganites [22]. The effect of NN and NNN Heisenberg couplings on the interplay of AFM and CO parameters is communicated [23].

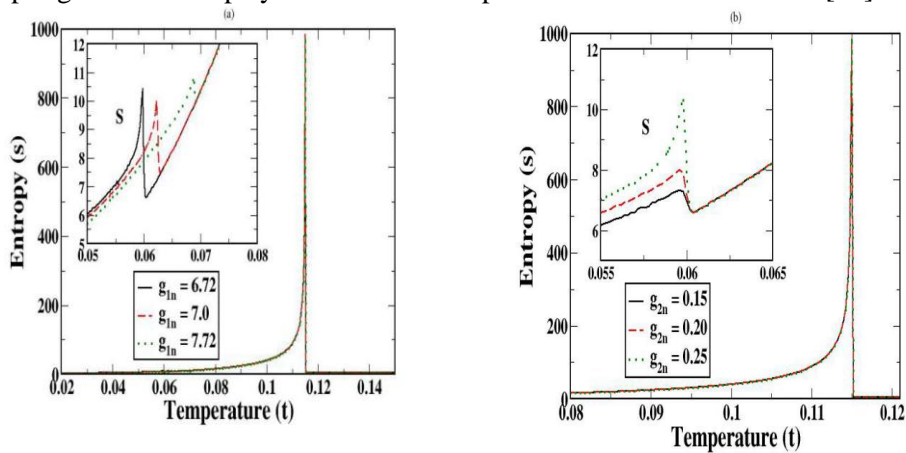


Fig. 3(a). The temperature dependent S for fixed values of $g = 1.08$, $g_1 = 2.5$, $g_{2n} = 0.25$, $t_2 = 0.075$ and different values of $g_{1n} = 6.72, 7.0, 7.72$. Inset: the magnified temperature dependent S for different values of g_{1n} . **(b)** Temperature dependent S for fixed values of $g = 1.08$, $g_1 = 2.5$, $g_{1n} = 6.72$, $t_2 = 0.075$ and different values of $g_{2n} = 0.15, 0.20, 0.25$. Inset: the magnified temperature dependent S for different values of g_{2n} .

The figure 3(a) shows the plot of the temperature dependent entropy for different NN Heisenberg coupling $g_{1n} = 6.72, 7.0, 7.72$. It is observed that the NN Heisenberg coupling has no effect on the entropy near charge ordering temperature (t_{CDW}). However, the entropy is suppressed with increase of NN heisenberg coupling below the spin ordering temperature (t_N). Further, the coupling g_{1n} enhances the Neel temperature. With increase of g_{1n} the jump in entropy becomes smaller and smaller. Figure 3(b) shows the effect of NNN Heisenberg coupling g_{2n} on entropy. The NNN Heisenberg coupling has no effect on entropy for temperature range $t_N \approx 0.06 < t < t_{CDW} \approx 0.116$ and also on charge ordering temperature. However the entropy is enhanced just below the Neel temperature for different NNN spin couplings with enhanced entropy jump near t_N . This indicates that NNN spin coupling (g_{2n}) plays a dominant role for the occurrence of CMR effect in manganites.

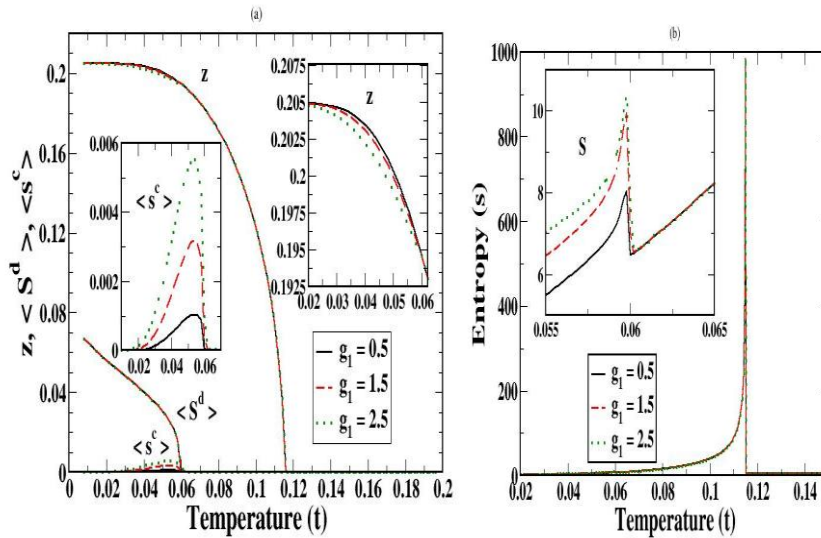


Fig. 4(a). The temperature dependent self-consistency graphs of z , $\langle S^d \rangle$ for fixed values of $g = 1.08$, $g_{1n} = 6.72$, $g_{2n} = 0.25$, $t_2 = 0.075$ and for different values of $g_1 = 0.5, 1.5, 2.5$. Inset: the temperature dependent self-consistency graph of $\langle S^c \rangle$ and z for different values of g_1 . **(b)** The temperature dependent S for fixed values of $g = 1.08$, $g_{1n} = 6.72$, $g_{2n} = 0.25$, $t_2 = 0.075$ and for different values of $g_1 = 0.5, 1.5, 2.5$. Inset: the temperature dependent S for different values of g_1 .

Figure 4(a) shows the plot of induced AFM spin fluctuation ($\langle s^c(t) \rangle$) for conduction electron which is computed by varying the DE coupling ($g_1 = 0.5, 1.5, 2.5$). The induced $\langle s^c(t) \rangle$ is enhanced with DE coupling near the Neel temperature (see inset of figure 4(a)). While the charge ordering is suppressed in the same temperature region exhibiting the interplay between charge ordering and spin ordering. It is to note that the magnetoresistivity in manganite systems appears near the magnetic ordering temperature. Figure 4(b) shows the plot of entropy for different DE coupling, $g_1 = 0.5, 1.5, 2.5$. The entropy (S) gradually increases from lower to higher temperatures, sharply increases to higher value and then sharply drops at charge ordering temperature $t_{CDW} \approx 0.116$. We observe another sharp drop in entropy at magnetic ordering temperature, $t_N = 0.06$. The entropy is enhanced with increase of DE coupling just below the Neel temperature. This may be related with increase of Linear specific heat coefficient (Υ) with increase of g_1 . Experimental findings give an increase of Υ for different manganite systems. For example $\Upsilon = 4.2\text{mJ/mole-K}^2$ for $\text{La}_{2/3}\text{C}_{1/3}\text{MnO}_3$ [24] and $\Upsilon = 9.3\text{mJ/mole-K}^2$ for $\text{La}_{0.2}\text{C}_{0.8}\text{MnO}_3$ [25] systems.

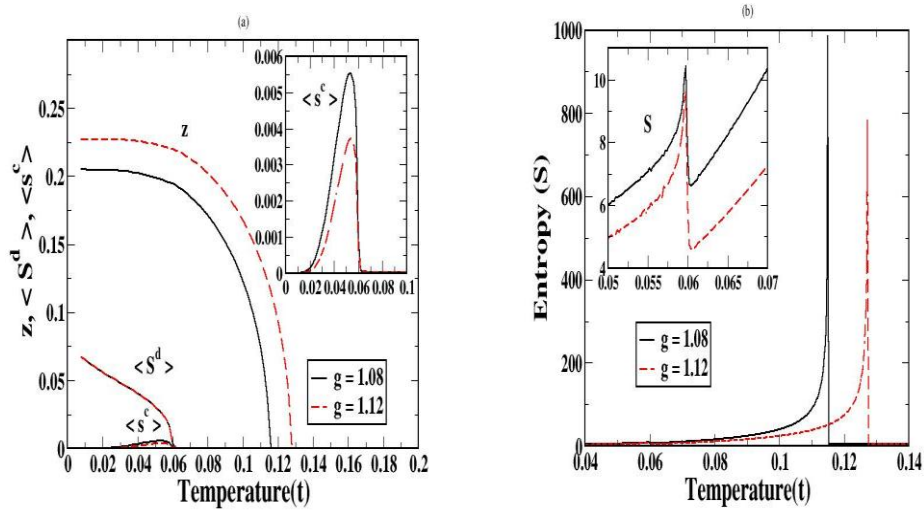


Fig. 5(a). The temperature dependent self-consistency graphs of $z, \langle S^d \rangle, \langle s^c \rangle$ for fixed values of $g_1 = 2.5, g_{1n} = 6.72, g_{2n} = 0.25, t_2 = 0.075$ and for different values of $g = 1.08, 1.12$. Inset: the temperature dependent self-consistency graph of $\langle s^c \rangle$. **(b)** Temperature dependent S for fixed values of $g_1 = 2.5, g_{1n} = 6.72, g_{2n} = 0.25, t_2 = 0.075$ and for different values of $g = 1.08, 1.12$. Inset: temperature dependent S for different values of g .

The effect of CDW coupling (g) on temperature dependent $z, \langle S^d(t) \rangle$ and $\langle s^c(t) \rangle$ is shown in figure 5(a). Increase of CDW coupling (g) increases CDW gap (z) throughout the temperature range as well as t_{CDW} shifts towards higher

temperature indicating involvement of more charges in the formation of CO state. As charge gets localized due to charge ordering, the magnetic ordering decreases with increase of g . This is reflected by suppression of $\langle s^c(t) \rangle$ in the temperature dependent $\langle s^c(t) \rangle$ curve. As CO state is formed in conduction band, the increase of g hardly affects spin fluctuation $\langle S^d(t) \rangle$ in core band. Also the Neel temperature remains unaltered. Suppression of $\langle s^c(t) \rangle$ just below t_N may lead to CMR effect. The effect of g on temperature dependent entropy is shown in figure 5(b). Increase of g suppresses the entropy throughout the temperature range. The entropy jump at t_{CDW} corresponding to CDW transition shifts to a higher temperature, while the magnetic jump at t_N does not shift.

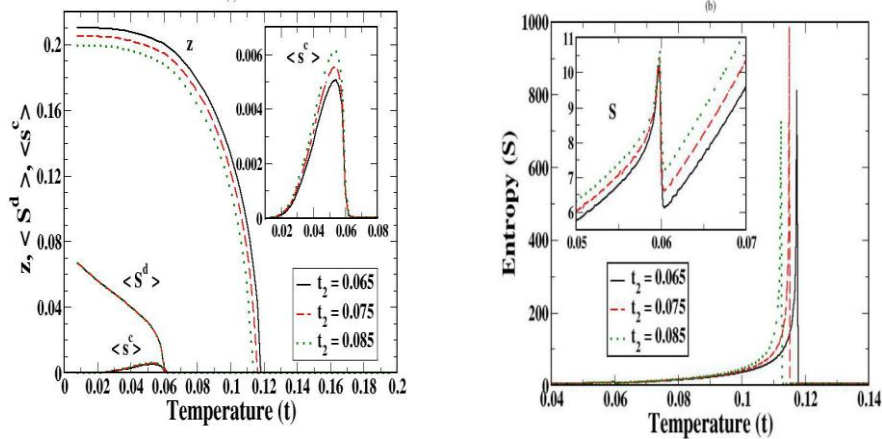


Fig. 6(a). The temperature dependent self-consistency graphs of z , $\langle S^d \rangle$ and $\langle s^c \rangle$ for fixed values of $g = 1.08$, $g_1 = 2.5$, $g_{1n} = 6.72$, $g_{2n} = 0.25$, and for different values of $t_2 = 0.065, 0.075, 0.085$. Inset: the temperature dependent self-consistency graph of $\langle s^c \rangle$ for different values of t_2 . **(b)** Temperature dependent S for fixed values of $g = 1.08$, $g_1 = 2.5$, $g_{1n} = 6.72$, $g_{2n} = 0.25$ and different values of $t_2 = 0.065, 0.075, 0.085$. Inset: temperature dependent S for different values of t_2

We also have studied the effect of second nearest neighbour hopping integral (t_2) on temperature dependent z , $\langle S^d(t) \rangle$ and $\langle s^c(t) \rangle$ as shown in figure 6(a). Increase of NNN hopping integral, t_2 increases the kinetic energy of the itinerant e_g electrons. So increase of t_2 suppresses CDW gap over the entire temperature range in CO phase, as formation of CO phase favours localization of charges. The AFM spin fluctuation $\langle s^c(t) \rangle$ in the same e_g band is enhanced below the Neel temperature, without changing the transition temperature. The $\langle S^d(t) \rangle$ is not affected by variation of t_2 . Effect of t_2 on entropy is shown in figure 6(b). The position of entropy jump at CDW transition shift towards lower temperatures with increase of t_2 . The position of magnetic jump remains

unchanged. But the entropy (S) increases just below and above t_N with increase of t_2 .

4. Conclusion

The calculations of induced c - electron spin fluctuation and the temperature dependent entropy and linear specific heat coefficient are strongly depend on the DE coupling, second nearest neighbour Heisenberg coupling and second nearest neighbour electron hopping integral. This displays a strong interplay between spin and charge orderings in manganite system, where CMR effect is prominent near the magnetic transition temperature. In another tight binding model calculation we have considered Jahn-Teller (as an extra mechanism of charge ordering distortion) for manganite system and its role on spin ordering. The calculations of spin fluctuation in core electrons and in e_g electrons, the lattice strain as well as the specific heat shows that NN and NNN Heisenberg spin coupling drastically changes both the magnitudes of lattice strain and spin orderings as well as the magnetic and lattice distortion temperatures. Using this model we have reported recently our studies on thermal properties like entropy and specific heat [26], and the temperature dependent tunneling conductance [27].

References

- [1] Y Tokura (Ed.) *colossal magnetoresistive oxides*, Gordon and Breach Science Publishers, Amsterdam, (2000)
- [2] C Zener, *Phys. Rev.* **81**,440 (1951); *ibid* **82**, 403 (1951)
- [3] K Kubo and N Ohata, *J. Phys. Soc. Jpn*, **33**, 21 (1972)
- [4] AJ Millis, B I Shraiman, and R Mueller, *Phys. Rev. B*, **54**, 5389 (1996)
- [5] A S. Alexandrov and A. M Bratkovsky, *Phys. Rev. Lett.*, **82**, 141 (1999); A. S Alexandrov, *J. Supercond. Nov. Magn.*, **22**, 95 (2009)
- [6] E Dagotto, *Nanoscale phase separation and colossal magnetoresistance*, Berlin, Germany; Springer, (2002); S. Dong, Q. Zhang, S. Yunoki, J. M. Liu and E. Dagotto, *Phys. Rev. B*, **86**, 205121 (2012)
- [7] G C Rout, N. Parhi and S. N Behera, *Physica B*, **404**, 2315 (2009)
- [8] G C Rout, S Panda and SN Behera, *J. Phys.: Condens. Matter*, **23**, 396001 (2011)
- [9] GC Rout, S Panda, S N Behera, *Physica B*, **404**, 4273 (2009)
- [10] GC Rout and S Panda, *Solid State Comm.*, **150**, 613 (2010)

- [11] G C Rout, S Panda and S N Behera, *J. Phys.: Condens. Matter* **22**, 376003 (2010)
- [12] G C Rout and S Panda, *J. Phys. Condens. Matter*, **21**, 416001 (2009)
- [13] S Panda, P K Purohit and G C Rout, *Phys., Express*, **3**, 30 (2013)
- [14] D N. Zubarev, *Sov. Phys. Usp.*, **3**, 320 (1960)
- [15] S Panda, J. K. Kar and G C Rout, *Mat. Res. Express*, **3**, 096104 (2016)
- [16] H Kuwahara et. al., *Phys. Rev Lett.* **82**, 4316 (1999)
- [17] S Okamoto et. al., *Phys. Rev. B*, **61**, 14647 (2000)
- [18] R K. Zheng, A N Tang, Y Yang, W Wang, G Li, X G Li and HC Ku, *J. Appl. Phys.* **94**, 514 (2003)
- [19] J Hejtmánek, Z Jiráček, Z Arnold, M Maryško, S Krupicka, C Martin and G Gorodetsky, *J. Appl. Phys.*, **107**, 063907 (2010)
- [20] KS Nagapriya, AK Raychaudhuri, B Bansal , V Venkataraman, S Parashar and CNR. Rao, *Phys. Rev. B*, **71**, 024426 (2005)
- [21] Y Tomioka , A Asamitsu ,H Kuwahara ,Y Moritomo and Y Tokura, *Phys. Rev. B*, **53**, R1689 (1996)
- [22] M Mochizuki, *Phys. Rev. B*, **80**, 134416 (2009)
- [23] J K Kar, S Panda and GC Rout, *AIP Conf. Proc.*, (2017) (In press)
- [24] Y Xu, J Zhang, G Cao, C Jing and S Cao, *Phys. Rev. B*, **73**, 224410 (2006)
- [25] V Markovich, J Wieckowski, M Gutowska, A Szewczyk, A Wisniewski, C Martin and G Gorodetsky, *J. Appl. Phys.*, **107**, 063907 (2010)
- [26] S Panda, N Santi, DD. Sahoo, GC Rout, *AIP Conf. Proc.*, (2017) (In press)
- [27] DD Sahoo, S Panda and GC Rout, *Orissa J. Phys.*, (2017) (communicated)